REPORT DOCUMENTATION PAGE	Form Approved OMB No. 0704-0188

PLEASE DO NOT RETURN YOUR FORM TO THE ABOVE ORGANIZATION.

1. REPORT DATE *(DD-MM-YYYY)*	2. REPORT TYPE	3. DATES COVERED *(From - To)*
03-08-2011	Conference Proceeding	

4. TITLE AND SUBTITLE
The Anatomy of Tubercles on Steel

5a. CONTRACT NUMBER

5b. GRANT NUMBER

5c. PROGRAM ELEMENT NUMBER
061153N

6. AUTHOR(S)
R.I. Ray, J.S. Lee, B.J. Little and T.L. Gerke

5d. PROJECT NUMBER

5e. TASK NUMBER

5f. WORK UNIT NUMBER
73-5052-10-5

7. PERFORMING ORGANIZATION NAME(S) AND ADDRESS(ES)
Naval Research Laboratory
Oceanography Division
Stennis Space Center, MS 39529-5004

8. PERFORMING ORGANIZATION REPORT NUMBER
NRL/PP/7330--10-0001

9. SPONSORING/MONITORING AGENCY NAME(S) AND ADDRESS(ES)
Office of Naval Research
800 N. Quincy St.
Arlington, VA 22217-5660

10. SPONSOR/MONITOR'S ACRONYM(S)
ONR

11. SPONSOR/MONITOR'S REPORT NUMBER(S)

12. DISTRIBUTION/AVAILABILITY STATEMENT
Approved for public release, distribution is unlimited.

13. SUPPLEMENTARY NOTES

14. ABSTRACT
The chemistry, mineralogy and microbiology of tubercles on cast iron and carbon steel were investigated. Tubercles, from diverse fresh water environments and of varying ages, consistently had an outer crust of geothite and lepidocrocite and an inner shell of magnetite. Core regions differed in structure, composition and chemistry. The presence of tubercles or a role for bacteria in their formation.

15. SUBJECT TERMS
microbiologically influenced corrosion, steel, freshwater, tubercles

16. SECURITY CLASSIFICATION OF:			17. LIMITATION OF ABSTRACT	18. NUMBER OF PAGES	19a. NAME OF RESPONSIBLE PERSON
a. REPORT	b. ABSTRACT	c. THIS PAGE			Richard Ray
Unclassified	Unclassified	Unclassified	UL	11	19b. TELEPHONE NUMBER *(Include area code)* 228-688-4690

Paper No.
11217

NACE® INTERNATIONAL CORROSION 2011 CONFERENCE & EXPO

THE ANATOMY OF TUBERCLES ON STEEL

R. I. Ray, J. S. Lee and B. J. Little
Codes 7332/7303
Naval Research Laboratory, Stennis Space Center, MS, USA, 39529

T. L. Gerke
Department of Geology, University of Cincinnati, Cincinnati, OH, USA, 45221

ABSTRACT

The chemistry, mineralogy and microbiology of tubercles on cast iron and carbon steel were investigated. Tubercles, from diverse fresh water environments and of varying ages, consistently had an outer crust of goethite and lepidocrocite and an inner shell of magnetite. Core regions differed in structure, composition and chemistry. The presence of tubercles on carbon steel and cast iron cannot be used to conclude localized corrosion directly under the tubercles or a role for bacteria in their formation.

Key words: microbiologically influenced corrosion, steel, freshwater, tubercles

INTRODUCTION

It is well established that tubercles formed on austenitic 300 series (304 or 316) stainless steel in untreated well water (200-300 ppm [Cl^-]) and chlorinated drinking water produce O_2 concentration cells and under-deposit corrosion. In an oxygenated environment, the area under the tubercle, deprived of O_2, becomes a relatively small anode compared to the large surrounding oxygenated cathode.[1-4] Metal is oxidized at the anode creating a pit and pH decreases. The pH in the pit depends on the alloying elements. Cl^- migrates from the electrolyte to the anode to neutralize charge, forming heavy metal chlorides that are extremely corrosive.[1-6] Pitting involves the conventional features of differential aeration, a large cathode: anode surface area and the development of acidity and metallic chlorides. Under these circumstances, the deposit or tubercle initiates the pitting and propagation is a function of alloy and environment (e.g., Cl^-). Tubercle formation on stainless steels is frequently[1-6] attributed to iron-oxidizing bacteria (IOB), e.g., *Gallionella* and *Leptothrix,* and the accumulation of bound oxidized iron. In summary, tubercles cause corrosion.

In contrast, tubercle formation on cast iron and carbon steel can be the result of corrosion, i.e., corrosion causes tubercles.[5] Throughout this paper the term "cast iron" specifically refers to unlined cast iron. Several authors have indicated a role for microorganisms in tubercle formation on

cast iron and carbon steels, especially IOB.[6] However, the relationships between tubercle formation, microorganisms and corrosion of cast iron and carbon steel in fresh water have not been established. In the following sections we present morphological, mineralogical, chemical and microbiological data for tubercles from three sources – Duluth-Superior Harbor (DSH), a fresh water estuary; a drinking water distribution system (DWDS) in the mid-western portion of the United States and a high-pressure industrial water system (HPIW) from a U.S. government facility located near the Gulf of Mexico.

METHODS AND MATERIALS

Details related to collection, embedding and imaging iron corrosion products have been reported elsewhere.[7] Operating conditions for the environmental scanning electron microscope (ESEM) and energy-dispersive spectroscopy (EDS) were described in the same publication.[7] The mineralogy of the tubercles was analyzed using a Siemens D-500 automated diffractometer system using a Cu Kα radiation at 30 mA and 40 kV. The 2θ ranged from 5° to 60°, with a 0.02° step, and a 2 second count time at each step. Crystalline phase identifications were made on the basis of peak position and peak intensities using the American Mineralogist Crystal Structure Database, the Mineral Database, and the International Center for Diffraction Data (http://rruff.geo.arizona.edu/AMS/amcsd.php, http://webmineral.com/). Approximately ten tubercles from each location were examined.

RESULTS

Tubercles from untreated fresh water in DSH

The water chemistry in DSH is as follows (concentrations in mg L^{-1}): pH, 7.8-9.4; DO, 4.4-11.7 (near saturation); sulfate (SO_4^{-2}), 4-30 and chloride (Cl^-), 10. DSH is icebound from mid-December to mid-April and during that time has a durable, well-defined ice cover. Freeze ice thicknesses in DSH range from 0.5 to 1.4 meters in addition to snow ice, stack ice, and ice from wave and splash action along harbor walls. Ice scour breaks and removes the tops of tubercles each year and tubercles reform within a few months.

DSH tubercles ranged in size from 2 x 3 cm after 1 year to 6 x 10 cm after 3 years. Tubercle height remained constant over the three-year period at about 2-5 mm. The general internal morphology of DSH tubercles consisted of a surface layer, overlying a hard shell layer that typically enclosed a core region (Figure 1). The surface layer of the DSH tubercles was made up of a reddish brown material composed of Fe(III) oxyhydroxides, primarily goethite with trace amounts of lepidocrocite. A black hard shell that had both metallic and non-metallic luster was under the surface layer and was composed predominantly of magnetite with trace amounts of goethite and lepidocrocite. The core region, yellowish-brown in color and composed of goethite and lepidocrocite, extended into the area of localized corrosion. Cores had a fibrous appearance and imaging with an ESEM demonstrated that the Fe(III) oxyhydroxides were associated with twisted bacterial stalks (Figure 2). Chromium, manganese and nickel were detected within the core regions. A feature of DSH tubercles is the well-defined stratum of copper at the base of the tubercles.

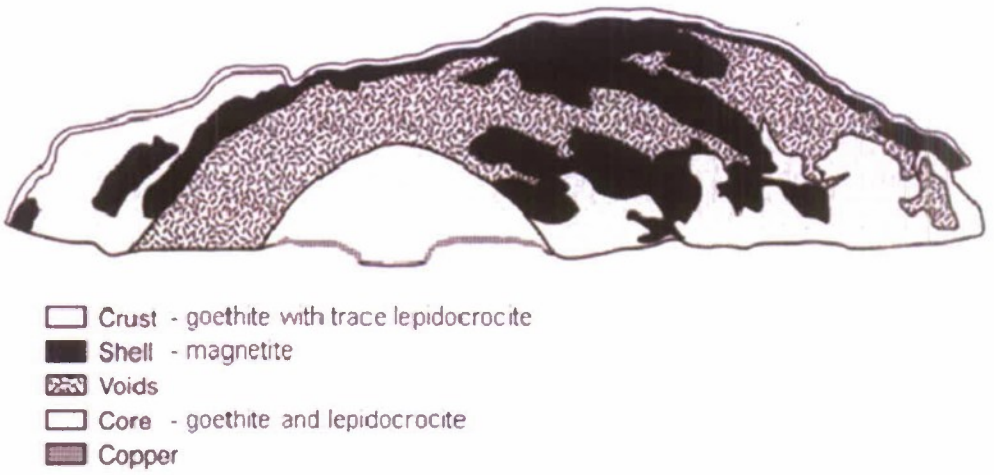

Figure 1. Diagram of DSH tubercle.

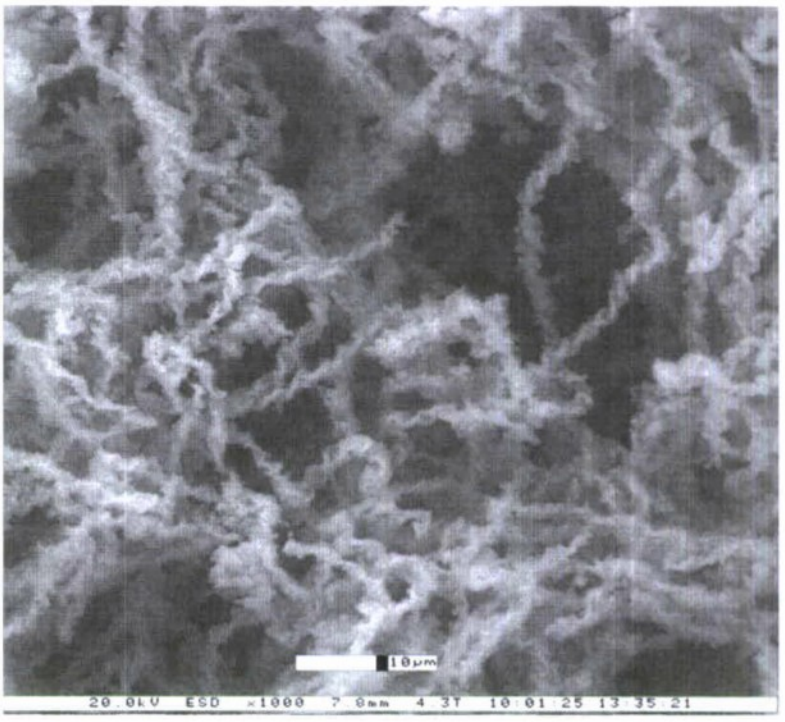

Figure 2. Twisted bacterial stalks with deposited iron within tubercle core from DSH.

All DSH tubercles were associated with localized corrosion, i.e., pitting (Figure 3). Pit volume, i.e., mass loss (depth x area) increased with time over a 3-year period. Average pit volumes (over a 625 mm^2 area) for year-1 and year-3 coupons were 86.12 mm^3 and 215.25 mm^3, respectively. Average pit depths for year-1 and year-3 coupons were 393.6 µm and 668.4 µm, respectively.

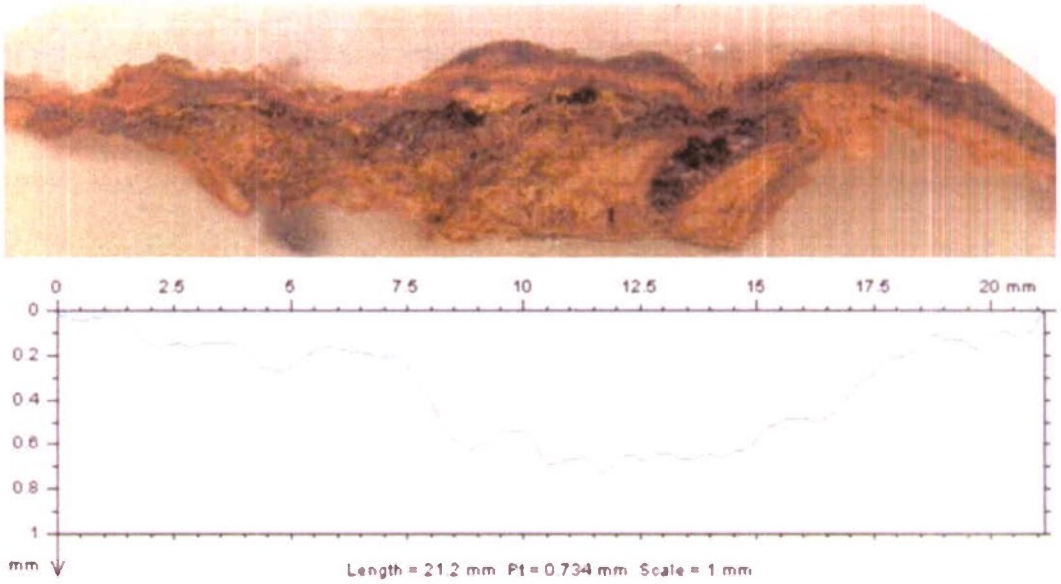

Figure 3. Cross section of tubercle and profile of pitting associated with DSH tubercle.

Tubercles from chlorinated DWDS

Tubercles removed from a 90 year-old cast iron pipe DWDS developed in water with the following composition (concentrations in mg L^{-1}): pH, 8.6, low to moderate hardness; alkalinity, 68; SO_4^{-2}, 98; free chlorine, 0.97 and phosphate, 0.083. The bulk water is oxygenated to saturation levels.

Tubercles from the DWDS ranged in size from a few to 10's of cm in length and in some locations had coalesced and were up to 100 cm long. An average tubercle was approximately 10 cm long and 5 cm high. The DWDS tubercles were not typically associated with localized corrosion (Figure 4). The general internal morphology of all tubercles examined from this DWDS consisted of a core region overlain by a hard shell and surface layer. Magnetite, lepidocrocite and goethite were the predominant iron minerals identified for the tubercles, but in different proportions.

Figure 4. Cross section of tubercle and cast iron pipe from DWDS.

Based on the different proportions of the iron phases in the core, tubercles were classified into three groups: Group 1a (goethite), Group 1b (lepidocrocite), and Group 2 (magnetite).[8] The predominant group, Group 1a, had core material that was yellowish- to reddish-brown in color and composed of goethite and trace amounts of lepidocrocite. This region was overlain by a black hard shell layer that has a metallic luster and was composed of magnetite with minor amounts of goethite and the surface layer was reddish in colored material composed primarily of goethite with minor amounts of lepidocrocite and magnetite. Magnetite veins were also present within the core regions of all tubercles in Groups 1a and 1b producing a marbled appearance and some contain sub-regions of filamentous textures. IOB could not be located within the core regions of tubercles from the DWDS.

Concentrations of phosphorus, calcium, lead, nickel, copper and zinc were detected by EDS throughout the core regions. Specific elements and concentrations of elements varied among tubercles from the same location and within a given region. In general the concentrations of calcium, copper, manganese, nickel, phosphorus, and zinc increased from the core to the surface layer. Aluminum concentrations were similar in the core and shell but increased in the surface layer. The highest concentrations of lead were localized in the surface layer and were lowest in the shell. Pitting was typically not associated with these tubercles (Figure 4).

Tubercles from high-pressure industrial water (HPIW)

The HPIW system is forty-three years old and the most recent water quality indicates the following (concentrations in mg L^{-1}): pH, 7.0, low to moderate hardness; SO_4^{2}, 12.2; chloride, 0.0. Tubercles were typically 5-10 cm long (developed along the axis of flow), 3-5 cm wide and 1-2 cm high. There were accumulations of lead within core regions. Tubercles from the HPIW had crusts of goethite and lepidocrocite and shells of magnetite. The core region contained biomineralized bacterial stalks (Figure 5). The tubercles were not associated with significant pitting.

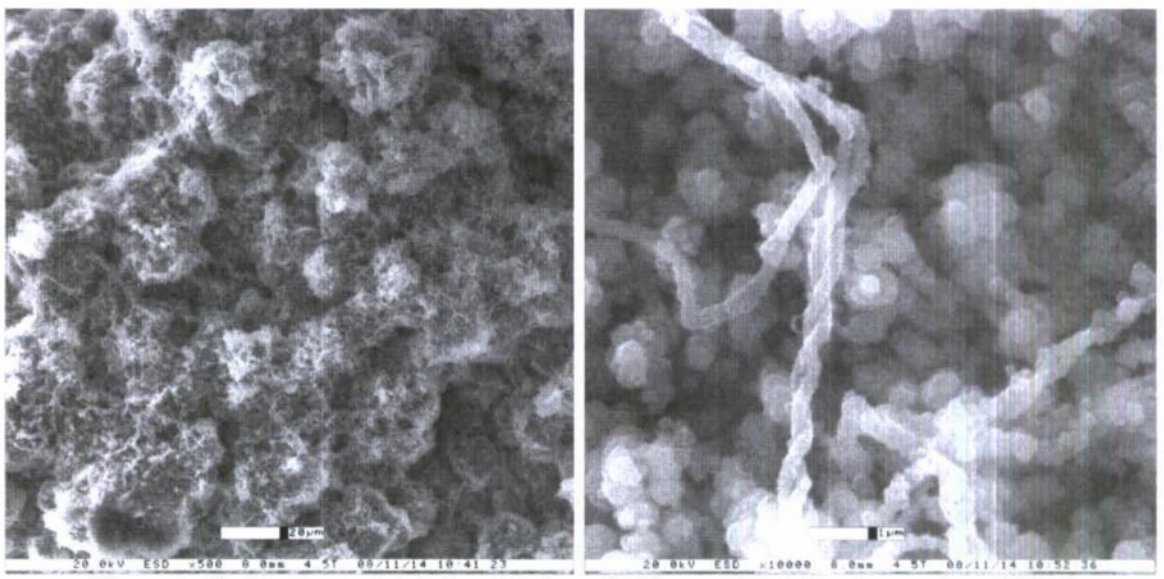

Figure 5. Twisted bacterial stalks with deposited iron within tubercle core from HPIW.

One tubercle was examined in detail. Based on its internal morphology it is similar to Group 1a discussed above. It had yellowish-brown colored core material composed of goethite and moderate amounts of lepidocrocite and veinlets composed of hard black non-metallic magnetite (Figure 6). This region was overlain by a black hard shell layer that has a metallic luster and was composed of magnetite with minor amounts of goethite and lepidocrocite. A very thin (less than 0.5

mm) thick surface layer overlies all and was reddish in colored material. Because this layer was so thin the mineralogy and chemistry could not be examined. Biomincralized bacterial stalks were located within the core region.

Concentrations of elements varied between the core and the hard shell layer of the representative tubercle. In general, concentrations of silicon, aluminum and sodium increased from the core to the hard shell layer and there was a slight increase from the core to the hard shell layer in calcium magnesium, and lead concentrations. The core had higher concentrations of iron and slightly higher phosphorous concentrations.

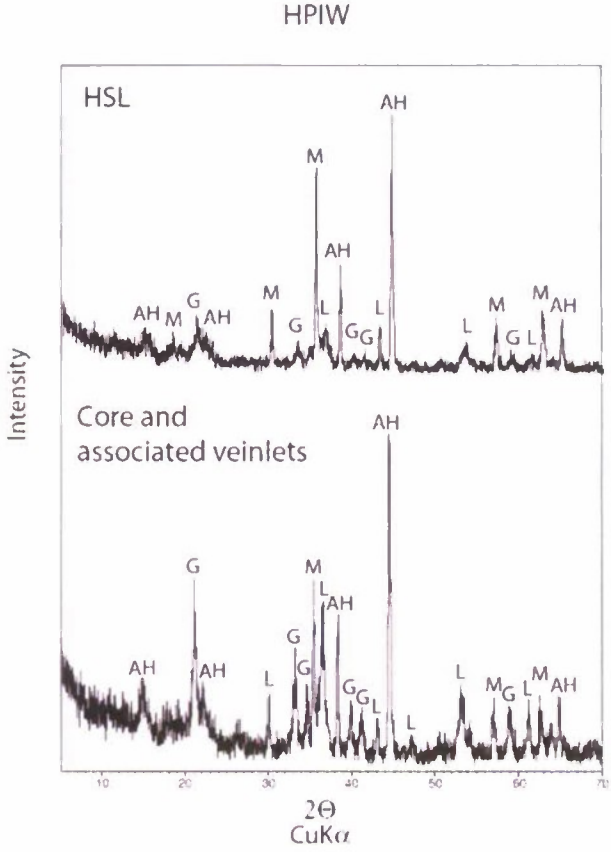

Figure 6. Powder X-ray diffraction patterns for the core and associated veinlets and hard shell layer (HSL) for a representative iron tubercle from HPIW. G = goethite (alpha-FeOOH), L = lepidocrocite (gamma-FeOOH), M = magnetite (Fe_3O_4), and AH = aluminum holder that the samples were analyzed.

DISCUSSION

Angell[5] described abiotic and biotic mechanisms for tubercle formation on carbon steel and cast iron, i.e., mounds of corrosion products deposited above areas of "localized electrochemical corrosion" and deposition of insoluble iron by IOB. Menzies[9] described abiotic tubercle formation at breaks or discontinuities in an oxide scale exposed in an oxygenated environment. "Anodic dissolution takes place and as metal ions concentrate in the solution the solubility product of the solid hydroxide is exceeded locally and hydroxide precipitates out as a hemispherical membrane which surrounds and covers the original discontinuity. This results in effective screening of the anodic area from available oxygen and the metal at the discontinuity remains anodic." Herro[10] working with tubercles in cooling waters concluded that differential aeration cells caused tuberculation, suggesting that oxygen deficient regions below the accumulated corrosion products were anodic sites, while

surrounding areas were cathodic. He indicated that tubercles grew as a result of both internal (anodic) and external (cathodic) reactions, i.e., anodic dissolution of metal resulted in the accumulation of Fe(II) (ferrous) and Fe(III) (ferric) ions and cathodic reactions outside the tubercle increased the pH and caused the precipitation of carbonate and other species whose solubility decreases with increasing pH.

Several investigators have demonstrated bacteria within tubercles.[7,11,12] Tuovinen and Hsu[13] suggested that there were zones within some tubercles that contained enough organic carbon and other nutrients to support the growth of microorganisms and microcosms with symbiotic relationships and nutrient cycling. Miller and Tiller[14] indicated, "iron bacteria, which, together with the ferric hydroxide they produce can form extensive deposits called tubercles on the inside of water pipes." Tiller[12] suggested that iron-oxidizing bacteria "encouraged" the formation of tubercles.

Several authors have described the internal morphologies of tubercles.[8,10,15] Herro[10] indicated that tubercles should contain the following structural features: outer crust (hematite, carbonate, silicates), inner shell (magnetite), core material (ferrous hydroxide, siderite, phosphates), fluid cavity and corroding floor. Sarin et al.[15,16] indicated a surface layer (lepidocrocite, $FeOH_3$, silicates, phosphates, carbonates), a shell-like layer (magnetite) and a porous core [Fe(II) and Fe(III) phases] over a corroding floor. The tubercles described in this paper, from three diverse locations, had the essential features described by previous models - core, shell and crust. The mineralogy of the crust and shell were identical to those described for tubercles isolated from other oxygen-saturated fresh water environments.

The significant difference between the Herro[10] and Sarin et al.[15,16] model is the absence of a fluid filled cavity in the Sarin et al.[15] model. Instead, Sarin et al.[15] suggested that porosity within the tubercle determined the ease with which ions migrate within the core. Their diagram indicated increased porosity at the base of the core. The cores described by Herro[10] and Gerke et al.[8] differed structurally and mineralogically. Gerke et al.[8] indicated that the majority of core material was Fe(III), either goethite or lepidocrocite, and Herro[10] described cores of Fe(II) hydroxide , siderite and phosphates. The cores from the tubercles in this study consistently contained a predominance of Fe(III) minerals, i.e., goethite and lepidocrocite.

In the present study, stalks produced by IOB and biomineralized deposits were located in tubercles from two locations – DSH and HPIW (Figures 2 and 5). Extracellular iron biomineralization has been studied extensively in fresh water.[17-20] Some iron-oxidizing microorganisms extrude polymeric structures upon which they deposit the ferric iron derived from their metabolism. Chan et al.[21] concluded that polymer directed iron hydroxide mineralization is a general phenomenon that can occur in any system containing acidic polysaccharides and iron. Banfield et al.[22] suggested that negatively charged polymers (e.g., *Gallionella* stalks) served as templates for aggregates of enzymatically produced iron oxides. Ghiorse and Ehrlich[23] suggested that microbial mineral formation can take place in intimate association with cells forming mineralized structures. They further concluded that the resulting structures could be used to identify a biological role in the formation in the absence of viable cells. Working with hyphal budding bacteria, Ghiorse and Hirsch[24] described the accumulation of positively charged iron hydroxides on negatively charged bacterial polymers. Once deposited, the iron oxides carried negative charges so that such a process could continue indefinitely without any biological activity. The only required biological input is the initial production of a negatively charged polymer. Sogaard et al.[25] described a similar process for biological iron precipitation by *Gallionella* in a polluted ground water (pH 5). Iron precipitated on the surface of the stalks until the negative charge effect was eliminated. The colloidal iron was condensed and the result was a dense deposit. Miot et al.[26] demonstrated precipitation of goethite on polymeric fibers extending from the cells of an iron-oxidizing bacterium. They also demonstrated a redox gradient, with the proportion of Fe(III) highest near the cells and the proportion of Fe(II) increasing at distance from the cell.

Bacteriogenic iron oxides, formed in response to chemical or bacterial oxidation of Fe(II) to Fe(III), are made up of intact and/or partly degraded remains of bacterial cells mixed with amorphous hydrous Fe(III) oxides.[27] Bacteriogenic iron oxides have reactive surfaces and act as sorbents of dissolved metal ions and enrichments of lead, cadmium, aluminum, chromium, zinc, manganese, and strontium, in addition to copper, have been reported.[28,29] Sarin et al.[15] reported the absorption of copper in iron corrosion scales. Gerke et al.[8] demonstrated that heavy metals, including copper, were either trapped within the structure or sorbed onto regions of the tubercles.

There were differences in the heavy metals associated with the cores varied with location and within locations. In the present study, heavy metals were co-located with bacteriogenic iron oxides in two locations (DSH and HPIW). Bacterial stalks were not identified in the fibrous core of DWDS tubercles but heavy metals were concentrated in the core regions. Chromium, manganese and nickel were detected within the core regions of DSH tubercles. A feature common to all DSH tubercles was a well-defined stratum of copper at the base of the tubercles. Concentrations of phosphorus, calcium, lead, nickel, copper and zinc were detected by throughout core regions of DWDS tubercles. There were accumulations of lead within core regions of HPIW tubercles. Specific elements and concentrations of elements varied among tubercles from the same location. These differences may reflect differences in heavy metal concentrations in the fresh water in which the tubercle develops. Because of the limited water quality data available from the locations examined in this study it is impossible to relate differences in core chemistry to water chemistry.

The Herro[10] and Sarin[15,16] models specifically describe tubercles associated with corrosion. Gerke et al.[8] described similar morphology, mineralogy and chemistry for tubercles developed in a DWDS, however, tubercles in the DWDS were not associated with localized corrosion. Angell[5] reported that the base of the tubercle was the source of "almost all of the iron that compromises the tubercle." Herro and Port[30] estimated that tubercle height was 5 to 30 times as great as the metal loss in the pit below. The Herro[10] model clearly does not describe the situation with any of the tubercles examined in this study. Tubercles formed in DSH must develop over warm summer months, are scrubbed from the surface by ice in the winter and early spring and reform. The height remained the same over a three-year period, despite the deepening pit beneath them. Tubercles in the DWDS and HPIW were not associated with localized metal loss. The cores of DSH tubercles extended into the pits and were exact replicas of the pit interior. Ray et al.[7] demonstrated that corrosion of pilings in DSH was due to a galvanic couple established between the copper layer and the iron substratum. The reducing conditions beneath the tubercles caused copper dissolved in the water to precipitate.

Data presented in this paper do not clarify the role of IOB in tubercle formation. Are IOB involved in tubercle formation or do tubercles in some environments provide conditions for IOB growth and biomineralization? Angell[5] suggested that tubercles provided anaerobic niches for sulfate reducing bacteria (SRB) and under some circumstances SRB could accelerate corrosion associated with tubercles. In an independent study, Lytle et al.[31] determined that some tubercles from the same DWDS examined in this study contained SRB.

CONCLUSIONS

The term "tubercle" does not describe a single morphology for corrosion products on carbon steel. The presence of tubercles on carbon steel cannot be used to conclude localized corrosion directly under the tubercles or a role for bacteria in their formation. The tubercles examined in this study did have features in common – a crust of lepidocrocite and goethite and a shell of magnetite. All tubercles had a core region, but the structure and chemistry of the cores differed. Stalks produced by iron-oxidizing bacteria were located in tubercles from two locations, but not the third.

ACKNOWLEDGEMENTS

This work was supported by the Office of Naval Research Program element 0601153N (6.1 Research Program), Dr. Linda Crisey at the Office of Naval Research (ONR Code 341) under award N0001410WX20247 and the U.S. Army Corps of Engineers, Detroit District. NRL Publication Number NRL/PP/7330-11-0001. We thank M. K. DeSantis for providing the digital images of the tubercle from the DWDS.

REFERENCES

1. B. J. Little, J. S. Lee, Microbiologically Influenced Corrosion (Hoboken, New Jersey: John Wiley and Sons, Inc., 2007).

2. S. W. Borenstein, P. B. Lindsay, "Microbiologically influenced corrosion failure analysis," Mater Performance 27, 3 (1988) p. 51-54.

3. G. Kobrin, "Corrosion by microbiological organisms in natural waters," Mater Performance 15 (1976) p. 38-43.

4. D. H. Pope, R. J. Soracco, E. W. Wilde, "Studies on biologically induced corrosion in heat exchanger systems at the Savannah River Plant, Aiken, SC," Mater Performance 21, 7 (1982) p. 43-50.

5. P. Angell, "Predictive model for non-microbiologically influenced corrosion tuberculation," Technical Report 1003442, Dec. 2003.

6. R. W. Lutey, "Identification and detection of microbiologically influennced corrosion," NSF-CONICET Workshop, Biocorrosion and Biofouling Proceedings (1992), p. 146-157.

7. R. I. Ray, J. S. Lee, B. J. Little, "Factors contributing to corrosion of steel pilings in Duluth-Superior Harbor," Corrosion 65, 11 (2009) p. 707-717.

8. T. L. Gerke, J. B. Maynard, M. R. Schock, D. L. Lytle, "Physiological characterization of five iron tubercles from a single drinking water distribution system: possible new insights on their formation and growth," Corros Sci 50 (2008) p. 2030-2039.

9. I. A. Menzies, "Introductory corrosion," in Microbial Aspects of Metallurgy, ed. J. D. A. Miller (New York, NY: American Elsevier Publishing Co., 1970), p. 35-60.

10. H. M. Herro, "MIC myths - does pitting cause MIC?," CORROSION / 98, 278 (Houston, TX: NACE International, 1998).

11. T. S. Rao, T. N. Sairam, B. Viswanathan, K. V. K. Nair, "Carbon steel corrosion by iron oxidising and sulphate reducing bacteria in a freshwater cooling system," Corros Sci 42, 8 (2000) p. 1417-1431.

12. A. K. Tiller, "Aspects of microbial corrosion," in Corrosion Processes, ed. R. N. Parkins (London & New York: Applied Science Publishers, 1982), p. 115-159.

13. O. H. Tuovinen, J. C. Hsu, "Aerobic and anaerobic microorganisms in tubercles of the Columbus, Ohio, water distribution-system," Appl Environ Microbiol 44, 3 (1982) p. 761-764.

14. J. D. A. Miller, A. K. Tiller, "Microbial corrosion of buried and immersed metal," in Microbial Aspects of Metallurgy, ed. J. D. A. Miller (New York, NY: American Elsevier Publishing Co., 1970), p. 61-105.

15. P. Sarin, V. L. Snoeyink, D. A. Lytle, W. M. Kriven, "Iron corrosion scales: Model for scale growth, iron release, and colored water formation," J Environ Eng-Asce 130, 4 (2004) p. 364-373.

16. P. Sarin, V. L. Snoeyink, J. Bebee, W. M. Kriven, J. A. Clement, "Physico-chemical characteristics of corrosion scales in old iron pipes," Water Res 35, 12 (2001) p. 2961-2969.

17. D. Fortin, S. Langley, A. Gault, A. Ibrahim, F. G. Ferris, I. D. Clark, "Stability of natural bacteriogenic iron oxides (BIOS) and their role in Sr cycling," Geochim Cosmochim Acta 72, 12 (2008) p. A278-A278.

18. R. E. James, F. G. Ferris, "Evidence for microbial-mediated iron oxidation at a neutrophilic groundwater spring," Chem Geol 212 (2004) p. 301-311.

19. C. S. Chan, G. De Stasio, S. A. Welch, M. Girasole, B. H. Frazer, M. V. Nesterova, S. Fakra, J. F. Banfield, "Microbial polysaccharides template assembly of nanocrystal fibers," Science 303, 5664 (2004) p. 1656-1658.

20. L. St.-Cyr, D. Fortin, P. G. C. Campbell, "Microscopic observations of the iron plaque of a submerged aquatic plant (Vallisneria-americana Michx)," Aquat Bot 46, 2 (1993) p. 155-167.

21. C. S. Chan, S. C. Fakra, D. C. Edwards, D. Emerson, J. F. Banfield, "Iron oxyhydroxide mineralization on microbial extracellular polysaccharides," Geochim Cosmochim Acta 73, 13 (2009) p. 3807-3818.

22. J. F. Banfield, S. A. Welch, H. Z. Zhang, T. T. Ebert, R. L. Penn, "Aggregation-based crystal growth and microstructure development in natural iron oxyhydroxide biomineralization products," Science 289, 5480 (2000) p. 751-754.

23. W. C. Ghiorse, H. L. Ehrlich, "Microbial biomineralization of iron and manganese," in Iron and Manganese Biomineralization Processes in Modern and Ancient Environments, Vol. Catena Supplement 21, eds. H. C. W. Skinner and R. W. Fitzpatrick (Cremlingen, Germany: Catena Verlag, 1992), p. 75-99.

24. W. C. Ghiorse, P. Hirsch, "Ultrastructural-study of iron and manganese deposition associated with extracellular polymers of pedomicrobium-like budding bacteria," Arch Microbiol 123, 3 (1979) p. 213-226.

25. E. G. Sogaard, R. Aruna, J. Abraham-Peskir, C. B. Koch, "Conditions for biological precipitation of iron by Gallionella ferruginea in a slightly polluted ground water," Appl Geochem 16, 9-10 (2001) p. 1129-1137.

26. J. Miot, K. Benzerara, M. Obst, A. Kappler, F. Hegler, S. Schadler, C. Bouchez, F. Guyot, G. Morin, "Extracellular Iron Biomineralization by Photoautotrophic Iron-Oxidizing Bacteria," Appl Environ Microbiol 75, 17 (2009) p. 5586-5591.

27. F. G. Ferris, "Biogeochemical properties of bacteriogenic iron oxides," Geomicrobiol J 22, 3&4 (2005) p. 79-85.

28. D. Dong, X. Hua, Y. Li, J. Zhang, D. Yan, "Cd adsorption properties of components in different freshwater surface coating:the important role of ferromanganese oxides," Environ Sci Technol 37, 18 (2003) p. 4106-4112.

29. R. E. Martinez, F. G. Ferris, "Review of the surface chemical heterogeneity of bacteriogenic oxides: proton and cadmium sorption," Am J Sci 305, 6 (2005) p. 854-871.

30. H. M. Herro, R. D. Port, NALCO Guide to Cooling Water System Failure Analysis (Boston: McGraw-Hill International, 1993).

31. D. A. Lytle, T. L. Gerke, J. B. Maynard, "Effect of bacterial sulfate reduction on iron-corrosion scales," J Am Water Works Ass 97, 10 (2005) p. 109-120.